Robotics and Autonomous Systems 62 (2014) 1305–1315

Contents lists available at ScienceDirect

Robotics and Autonomous Systems

journal homepage: www.elsevier.com/locate/robot

Passivity-based adaptive backstepping control of quadrotor-type UAVs[☆]

ChangSu Ha [a], Zhiyuan Zuo [b], Francis B. Choi [a], Dongjun Lee [a,*]

[a] Department of Mechanical & Aerospace Engineering and IAMD, Seoul National University, Seoul, 151-744, Republic of Korea

[b] Department of Mechanical, Aerospace & Biomedical Engineering, University of Tennessee, Knoxville, TN 37996, USA

HIGHLIGHTS

- Novel passivity-based adaptive backstepping control of under-actuated quadrotors.
- Demonstrated for the velocity field and trajectory tracking control of the quadrotors.
- Applied for stable haptic teleoperation of the quadrotor over the Internet.

ARTICLE INFO

Article history:
Available online 13 April 2014

Keywords:
Adaptive control
Backstepping
Internet
Passivity
Quadrotors
Teleoperation

ABSTRACT

We propose a novel unified passivity-based adaptive backstepping control framework for "mixed" quadrotor-type unmanned aerial vehicles (UAVs), which consists of the translation dynamics with thrust force input $\lambda \in \Re$ and the attitude kinematics with the angular velocity input $w \in \Re^3$ evolving on SE(3). We also show how our proposed unified framework can be used for velocity field following, timed trajectory tracking and haptic interaction over the Internet, while also providing a complete stability (or collision avoidance) analysis. Experiments using a real quadrotor and lossy communication (for the teleoperation) are also performed to illustrate the theory.

1. Introduction

Unmanned aerial vehicles (UAVs) are promising to achieve many useful applications with the cost associated to the on-board human pilots removed: landscape survey, entertainment and games, surveillance/reconnaissance, remote repair, and precise unmanned attack, to name a few. In particular, quadrotor-type UAVs have recently received much attention, due to its agility, (relative) easiness of control, affordability and availability [1]. Teleoperation of such quadrotors would even further expand the application horizons of this versatile flying robotic platform, particularly when it is required to perform complicated/cognitively-loaded tasks in uncertain/unknown environments [2–4].

In this paper, we propose a novel adaptive backstepping control framework for "mixed" quadrotor-type UAVs [5], which can be modeled as a combination of the translation dynamics in E(3) and the attitude kinematics in SO(3), with the thrust force $\lambda \in \Re$ and the angular velocity $w \in \Re^3$ as the control input. Here, we focus on these "mixed" quadrotors, since: (1) many commercially available UAVs (e.g., Asctec Hummingbird® or Pelican®) often allow for direct control of only its angular velocity, not the angular torque, and (2) it is usually possible to design (low-level) angular torque input (i.e., for attitude dynamics) to duplicate (high-level) angular velocity command for the quadrotor's fully-actuated rotation dynamics, thereby, can "modularize" rotational control implementation.

This mixed quadrotor, however, is under-actuated with only the 1-degree-of-freedom (DOF) thrust force input λ for the 3-dimensional Cartesian dynamics in E(3), although the rotational dynamics in SO(3) is fully-actuated with $w \in \Re^3$. On the other hand, the mass parameter of the quadrotor as regards to the thrust force λ in general suffers from some uncertainty, particularly due to many nonlinear effects on the generation mechanisms of λ.

In this paper, we propose a novel unified passivity-based adaptive backstepping control framework for the mixed quadrotors, where the backstepping technique [6] is used to overcome the quadrotor's under-actuation, while the parameter adaptation approach to online estimate uncertain mass parameter of the quadrotor [7]. For this, we particularly reveal and utilize a certain passivity

☆ Research supported in part by the Korea National Research Foundation (Ministry of Education, Science and Technology) under the Grants 2012-R1A2A2-A01015797 and 2009-0087640, and the US National Science Foundation under the Grant CMMI-0727480.

* Corresponding author.
E-mail address: djlee@snu.ac.kr (D. Lee).

http://dx.doi.org/10.1016/j.robot.2014.03.019
0921-8890/

structure inherent to this quadrotor-type UAV. Moreover, we also characterize a class of control actions, which are designed for the fully-actuated point-mass dynamics, yet, still transferable to the under-actuated quadrotors with uncertain mass parameter. This unified class of control actions in fact includes the following two possibly most widely-used control objectives: velocity field following and timed trajectory tracking. We also show how our adaptive backstepping trajectory tracking control can be applied to the recently proposed semi-autonomous teleoperation control architecture in [2] and also provide a complete stability and collision avoidance analysis of the total teleoperation-loop.

Numerous strong control techniques have been proposed for the control of quadrotors or similar systems (e.g., [8–14]). However, they are typically developed for specific control objectives (e.g., trajectory tracking [5,8,9,11,13,14]; path or velocity following [10,13]) and do not aim to provide a unified control synthesis framework or characterize the class of possible control actions as achieved in this paper. Most of the available results for the quadrotor control is also for dynamic quadrotors (i.e., accept thrust force and angular torque input) even if many commercially-available systems are "mixed" quadrotors (i.e., accept thrust force and angular velocity input). In contrast, our proposed adaptive backstepping control framework is derived specifically for these "mixed" quadrotors, thus, applicable to many such commercial quadrotor platforms and also much simpler (and easier to implement) than those control laws developed for dynamic quadrotors (cf., [9,10,14]). Our backstepping control also fully embraces the geometry of SE(3), thus, free from the singularity stemming from SO(3) parameterization (e.g., [11,12]), and on-line adapts the mass parameter of the quadrotors, which turn out to be crucial to maintain desired height in real implementation (cf., [9]).

We also show how to apply our adaptive backstepping control to the recently proposed UAV teleoperation architecture of [2]. For this, we particularly elucidate how to utilize a dynamic-extension like filter to circumvent the problem of using high-order derivatives of the master device's position signal received from the discontinuous Internet for our adaptive backstepping control; provide a complete stability/collision-avoidance analysis including all the control-layers in the teleoperation architecture; and also present new Internet teleoperation experimental results with lossy-communication, all of which were only alluded or missing in [2].

A conference version of this paper is [15]. However, in [15], only the backstepping trajectory tracking control (i.e., result of Section 3.2) was presented with no parameter adaptation and robustness analysis. The current version generalizes the result of [15] to the unified passivity-based adaptive backstepping control design while also characterizes a class of possible control actions, with the trajectory tracking in [15] merely as one example of such. The proof of stability/collision-avoidance for the teleoperation (i.e., Proposition 1) is also completely revised to fully incorporate all the relevant control layers. All new experiments are also performed, particularly those on teleoperation with lossy-communication presented for the first time here.

The rest of this paper is organized as follows. Section 2 presents the modeling of the "mixed" quadrotors. Our unified passivity-based adaptive backstepping control framework for quadrotors is then presented and detailed in Section 3 along with velocity following (Section 3.1) and trajectory tracking (Section 3.2) as examples for that. We then apply our adaptive backstepping tracking control for the problem of haptic teleoperation over the Internet in Section 4. Experimental results are then presented in Section 5. Some concluding remarks are given in Section 6.

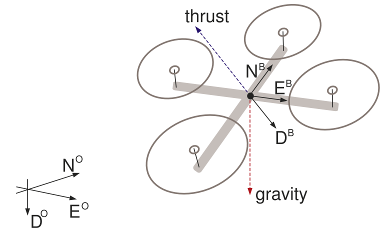

Fig. 1. Quadrotor: $\{O\} := \{N^o, E^o, D^o\}$ and $\{B\} := \{N^B, E^B, D^B\}$ are the inertial and body frames, with thrust and gravity along D^B and D^o.

2. Under-actuated quadrotor-type UAV

We consider the following quadrotor-type UAV, evolving on SE(3) according to the translation dynamics and attitude kinematics [5,13]:

$$m\ddot{x} = -\lambda Re_3 + mge_3 + \delta \tag{1}$$

$$\dot{R} = RS(w) \tag{2}$$

where $m > 0$ is the (uncertain) mass, $x \in \Re^3$ is the Cartesian position expressed in the inertial NED (north-east-down) frame with e_3 representing its down-direction, $\lambda \in \Re$ is the thrust along the body-frame down direction, $\delta \in \Re^3$ is the Cartesian disturbance, $R \in SO(3)$ is the rotational matrix describing the orientation of the body NED frame of UAV relative to the inertial NED frame, $w := [w_1, w_2, w_3] \in \Re^3$ is the angular velocity of the UAV expressed in the body NED frame, g is the gravitational constant, and $S(\star) : \Re^3 \to so(3)$ is the skew-symmetric operator defined s.t. for $a, b \in \Re^3$, $S(a)b = a \times b$. See Fig. 1.

Here, we assume that the control inputs for the quadrotor (1)–(2) are the thrust force $\lambda \in \Re$ and the angular velocity $w \in \Re^3$. This "mixed" quadrotor (1)–(2) can capture many commercially available UAVs shipped with a manufacturer's low-level attitude control servo-loop already implemented (e.g. Asctec Hummingbird®). The control inputs (λ, w) obtained for these "mixed" quadrotors (1)–(2) can also be applied to the "dynamic" quadrotors (i.e., with translation and attitude dynamics). This is because it is rather straightforward to design the angular torque input $\tau \in \Re^3$ for the dynamic quadrotors to reproduce the target angular velocity w, as its rotational dynamics on SO(3) is fully-actuated (e.g., passivity-based control [16]).

The main difficulty of controlling the quadrotor-type UAV (1)–(2) is that it is under-actuated, that is, although the rotation motion can be directly driven by $w \in \Re^3$, its Cartesian dynamics (1) has only 1-DOF thrust input λ, whose direction is fixed along the down-direction of the UAV's body and can only be controlled via its rotational motion. In Section 3, we will show that, even with this issue of under-actuation and also with uncertainty in the estimate of quadrotor's mass m, a fairly large class of control actions, which can be achieved for the simple point-mass dynamics (i.e., $m\ddot{x} = u$), can also be attained for the quadrotor's Cartesian motion (1). For this, we will utilize the backstepping technique [6] along with adaptive control approach [7] to respectively address the issues of the under-actuation and the parametric uncertainty in m, while also exploiting a certain passivity property of the under-actuated quadrotors (1)–(2) with some suitably defined input–output pairs.

3. Unified passivity-based adaptive backstepping control of quadrotor UAVs

Suppose we want the quadrotor's Cartesian position $x \in \Re^3$ to evolve according to a certain desired control $\nu \in \Re^3$ with the target closed-loop dynamics of x given by

$$m\ddot{x} = \nu(m, x, \dot{x}, t) \tag{3}$$

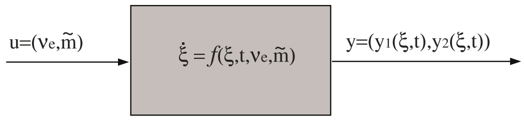

Fig. 2. Passivity of the closed-loop quadrotor Cartesian dynamics with under-actuation and uncertain mass parameter m (see (9)).

where $\nu(m, x, \dot{x}, t)$ is the control designed for the point-mass dynamics while ignoring the issue of the quadrotor's under-actuation. Here, we assume ν to be a function of x, $\dot{x}$ and the time t, and also requires the mass m of the quadrotor. We also assume that the target closed-loop dynamics (3) can be written as the following dynamics equation

$$\dot{\xi} = f_o(\xi, t) \tag{4}$$

where $\xi \in \Re^m$ constitutes the state of the closed-loop dynamics (3) and $f_o : \Re^m \times \Re^+ \to \Re^m$ has its equilibrium at $\xi = 0$ and defines an asymptotically stable dynamics around this equilibrium. We further assume that the equilibrium of the closed-loop dynamics (3) (or (4)) defines the desired behavior for x, that is, what we want to achieve is

$$\xi \to 0 \tag{5}$$

(e.g., $\xi = (x, \dot{x})$ for stabilization).

Of course, due to the under-actuation of the quadrotor, it is in general impossible to duplicate the desired control ν by the thrust-input $\lambda R e_3$ in (1), as its direction (i.e., Re_3) can be controlled only through the rotational motion (2), although its magnitude (i.e., λ) can be directly assignable. On top of this, the mass parameter m is also in general uncertain. This then means that, instead of implementing the ideal control $-\lambda R e_3 = -mge_3 + \nu(m, x, \dot{x}, t)$ to attain the target dynamics (3), we rather would merely be able to implement the following control action

$$-\lambda R e_3 = -\hat{m} g e_3 + \nu(\hat{m}, x, \dot{x}, t) + \nu_e \tag{6}$$

where $\hat{m} > 0$ is the estimate of the m, and $\nu_e \in \Re^3$ is the control generation error due to the quadrotor's under-actuation. The closed-loop dynamics of the quadrotor then becomes

$$m\ddot{x} = \nu(\hat{m}, x, \dot{x}, t) + \tilde{m} g e_3 + \nu_e \tag{7}$$

instead of (3), where

$$\tilde{m} := m - \hat{m}$$

is the mass estimation error.

Similar to (4), now, we suppose that this "real" closed-loop dynamics (7), under the parameter uncertainty and the quadrotor's under-actuation, can also be written as the following dynamics equation

$$\dot{\xi} = f(\xi, t, \nu_e, \tilde{m}) \tag{8}$$

where $f : \Re^m \times \Re^+ \times \Re^3 \times \Re \to \Re^m$ defines the dynamics with its asymptotically stable equilibrium at $\xi = 0$ when $(\nu_e, \tilde{m}) = 0$. We further assume that this dynamics (8) possesses the following (strict state) passivity property with $(\nu_e, \tilde{m}) \in \Re^4$ as its input and $y(\xi, t) = (y_1(\xi, t), y_2(\xi, t)) \in \Re^4$ as its output [17]:

$$\frac{dW_1}{dt} = -\xi^T Q \xi + y_1^T(\xi, t)\nu_e + y_2(\xi, t)\tilde{m} \tag{9}$$

where $W_1 := \frac{1}{2}\xi^T P \xi$ is a storage (or Lyapunov) function with $P, Q \in \Re^{m \times m}$ being positive-definite and symmetric matrices. See Fig. 2. This passivity property (9) turns out to be crucial for our design of adaptive backstepping control as follows.

Now, let us augment the storage function W_1 s.t.

$$W := W_1 + \frac{1}{2\gamma_1}\nu_e^T \nu_e + \frac{1}{2\gamma_2}\tilde{m}^2$$

where $\gamma_1, \gamma_2 > 0$ are the gains. Differentiating this W, we obtain

$$\frac{dW}{dt} = -\xi^T Q \xi + y_1^T \nu_e + y_2 \tilde{m} + \frac{1}{\gamma_1}\nu_e^T \dot{\nu}_e - \frac{1}{\gamma_2}\tilde{m}\dot{\hat{m}}$$

with $\dot{\tilde{m}} = -\dot{\hat{m}}$ from m being a constant. This then suggests the following backstepping and adaptation laws:

$$\dot{\nu}_e = -\gamma_1 y_1(\xi, t) - \alpha \nu_e \tag{10}$$

$$\dot{\hat{m}} = \gamma_2 y_2(\xi, t) \tag{11}$$

where $\alpha > 0$ is the backstepping gain. With these backstepping and adaptation laws (10)–(11), we then have

$$\frac{dW}{dt} = -\xi^T Q \xi - \alpha \nu_e^T \nu_e \le 0$$

implying that W is bounded, and so are ν_e, ξ and $\tilde{m}$.

Moreover, from Barbalat's lemma [16], we can also show that, if $\dot{\xi}$ and $\dot{\nu}_e$ are bounded, $\dot{W} \to 0$. For this, we assume that $f(\xi, t, \nu_e, \tilde{m})$ and $y_i(\xi, t)$ are bounded, if ξ, ν_e, $\tilde{m}$ are bounded. These assumptions then imply that $\dot{\xi}$ in (8) and $\dot{\nu}_e$ in (10) are bounded, as the boundedness of ξ, ν_e, $\tilde{m}$ have already been established above. With $\dot{W} \to 0$, we can then conclude that $(\xi, \nu_e) \to 0$, meaning that the control objective (5) is granted with the control generation error ν_e also vanishing, even though the system is under-actuated with parametric uncertainty in m, The parameter convergence of $\tilde{m}$ can also be achieved under the standard persistence of excitation condition [16].

Although the adaptation law (11) can be directly implemented (i.e., integrated in software), the backstepping law (10) must be "decoded" into the real control inputs λ and w in (1)–(2). For this, similar to [5], differentiating (6) with (2), the following decoding relation can be obtained

$$[(\dot{\lambda} + \alpha\lambda)R + \lambda R S(w)]e_3 = \bar{\nu}$$

where

$$\bar{\nu} := -\left[\frac{d}{dt} + \alpha\right]\left[\nu(\hat{m}, x, \dot{x}, t) - \hat{m} g e_3\right] + \gamma_1 y_1(\xi, t). \tag{12}$$

By using the structure of the skew-symmetric $S(w)$, the above equation can be simplified s.t.

$$\begin{pmatrix} \lambda w_2 \\ -\lambda w_1 \\ \dot{\lambda} + \alpha\lambda \end{pmatrix} = R^T \bar{\nu}. \tag{13}$$

We can then compute the control inputs (λ, w_1, w_2) from (13) as follows: (1) compute w_2, w_1 by dividing the first and second rows of the RHS of (13) by λ if $\lambda \neq 0$, and (2) integrate λ by solving the differential equation in the last row of (13). Assuming $\lambda \neq 0$ (to obtain w_1, w_2) is typical for quadrotor control (i.e., no free-fall [8–10]). Note from (13) that, for the Cartesian position x control, we only need λ, w_1 and w_2, yet, not w_3. This is again typical for the quadrotor control [8–10]. We may simply set $w_3 = 0$ or use it for other purpose (e.g., on-board camera pointing operation). By considering the attitude kinematics with a certain low-level angular velocity tracking controller assumed, our control decoding equation (13) is substantially simpler (thus, easier to implement in practice) than that in [9,10], which is based on the full attitude dynamics.

The following Theorem 1 summarizes our design of passivity-based adaptive backstepping control so far. The parameter convergence of $\hat{m}$ in Theorem 1 is also due to the standard persistency of excitation argument of adaptive control [16].

Theorem 1. *Consider the quadrotor (1)–(2) with the passivity property (9) and $\delta \approx 0$ under the backstepping and adaptation laws (13) and (11). Then, $(\xi, \nu_e, \tilde{m})$ is bounded $\forall t \geq 0$. Suppose also that $f(\xi, t, \nu_e, \tilde{m})$ and $y_i(\xi, t)$ are bounded if $\xi, \nu_e, \tilde{m}$ are bounded. Then, $(\xi, \nu_e) \to 0$. Furthermore, suppose that $y_2(\xi, t) \in \Re$ can be parameterized s.t.*

$$y_2(\xi, t) = \xi^T \Gamma Y_2(t) \tag{14}$$

with $\Gamma \in \Re^{m\times m}$. Then, $\hat{m} \to m$, if the following persistence of excitation condition holds: $\exists$ strictly positive $\varepsilon, T > 0$ s.t.,

$$\int_t^{t+T} Y_2^T(\tau)\Gamma^T \Gamma Y_2(\tau) d\tau \geq \varepsilon$$

for all $t \geq 0$.

Note that the backstepping control (13) requires an access to the quadrotor's Cartesian acceleration $\ddot{x}$ due to the presence of the term $\frac{d}{dt}\nu(\tilde{m}, x, \dot{x}, t)$ in (12). For this, we may use an on-board accelerometer to directly measure $\ddot{x}$, which is typically installed on most of commercial quadrotor platforms; or, as suggested in [5], use the dynamics equation itself (1) to obtain the estimate of $\ddot{x}$ s.t.

$$\hat{\ddot{x}} := -\frac{\lambda}{\hat{m}} Re_3 + ge_3 \tag{15}$$

where $\hat{m}$ is the adaptive estimate of m, which is typically projected to a certain strictly-positive interval reflecting the likely value of m (i.e., $\hat{m} \in [\underline{m}, \overline{m}]$, $0 < \underline{m} \leq m \leq \overline{m}$).

From our experience, we found that, particularly when the disturbance δ in (1) is small (e.g., quadrotor flies indoor with no physical interaction with human/environment), this usage of dynamics equation to estimate $\ddot{x}$ in (15) is often adequate and outperforms the usage of accelerometer, which suffers from noise and bias. The following Lemma 1 further justifies our usage of the dynamics equation to estimate $\ddot{x}$ by showing the robustness of our control scheme against the bounded error in the acceleration estimation.

Lemma 1. *Consider the quadrotor (1)–(2) with the passivity property (9) and $\delta \approx 0$ under the backstepping and adaptation laws (13) and (11). Suppose that $\tilde{m}$ and $\frac{\partial \nu(\hat{m},x,\dot{x},t)}{\partial \dot{x}}$ are bounded, and $y_2(\xi, t)$ is linearly-parameterizable as given in (14) with bounded $Y_2(t)$. Then, if the acceleration estimation error $\tilde{\ddot{x}} := \ddot{x} - \hat{\ddot{x}}$ is bounded, (ξ, ν_e) is ultimately bounded* [17].

Proof. The acceleration estimate error $\tilde{\ddot{x}}$ perturbs the expression of (12) s.t.,

$$\bar{\nu} = -\left[\frac{d}{dt} + \alpha\right]\left[\nu - \hat{m}ge_3\right] + \gamma_1 y_1(\xi, t) + \frac{\partial \nu}{\partial \dot{x}}\tilde{\ddot{x}}$$

and, consequently, the backstepping law (10) is also perturbed by

$$\dot{\nu}_e = -\gamma_1 y_1 - \alpha \nu_e - \frac{\partial \nu}{\partial \dot{x}}\tilde{\ddot{x}}$$

where arguments are omitted for brevity. Define

$$W' := W_1 + \frac{1}{2\gamma_1}\nu_e^T \nu_e$$

with $W_1 = \frac{1}{2}\xi^T P \xi$ is positive definite. We can then show that, using (14),

$$\frac{dW'}{dt} = -\xi^T Q \xi - \alpha \nu_e^T \nu_e + \xi^T \Gamma Y_2 \tilde{m} - \frac{1}{\gamma_1}\nu_e^T \frac{\partial \nu}{\partial \dot{x}}\tilde{\ddot{x}} \tag{16}$$

which shows the ultimated boundedness of (ξ, ν_e), as the first two terms on the RHS define exponential stability of (ξ, ν_e), while the other two terms are linear in (ξ, ν_e) with other terms there bounded. ■

This Lemma 1 then shows that, even if the acceleration estimate $\hat{\ddot{x}}$ is imprecise (e.g., by using dynamics equation), the states will be eventually bounded and stay bounded thenceforth. Of course, the more precise the acceleration estimate $\hat{\ddot{x}}$ gets, the closer the quadrotor's behavior converges to the desired one as specified in Theorem 1. In the next two subsections, we will provide examples of our passivity-based adaptive backstepping control for the two important control objectives, namely, velocity field following (Section 3.1) and timed-trajectory tracking (Section 3.2).

3.1. Example 1: velocity field following

Let us define a vector field V on the Cartesian position x of the quadrotor (1)–(2)

$$V : x \in \Re^3 \mapsto V(x) \in \Re^3$$

where $V(x)$ defines the desired velocity at the Cartesian position x. The control objective is

$$\dot{x} \to V(x)$$

as $t \to \infty$. To achieve this velocity field following, similar to (6), we design the control action s.t.,

$$-\lambda Re_3 := -\hat{m}ge_3 + \underbrace{\hat{m}\dot{V} - b(\dot{x} - V)}_{=:\nu(\hat{m},x,\dot{x},t)} + \nu_e \tag{17}$$

where $b > 0$ is the control gain and $\dot{V} := \frac{\partial V}{\partial x}\dot{x}$, with the ij-th component of $\frac{\partial V}{\partial x} \in \Re^{3\times 3}$ given by $\frac{\partial V}{\partial x}\big|_{ij} = \frac{\partial V_i}{\partial x_j}$.

Injecting this control (17) to (1) with $\delta \approx 0$, we can obtain the closed-loop Cartesian dynamics s.t.,

$$m\dot{e}_v + be_v = \tilde{m}(ge_3 - \dot{V}) + \nu_e$$

where $e_v := \dot{x} - V$. We can further show that this closed-loop dynamics satisfies the passivity property (9) with $\xi = e_v \in \Re^3$ and $W_1 = \frac{1}{2}m\xi^T\xi$, that is,

$$\frac{dW_1}{dt} = -be_v^T e_v + e_v^T \nu_e + \tilde{m}e_v^T(ge_3 - \dot{V})$$

with $y_1 = e_v$ and $y_2 = e_v^T(ge_3 - \dot{V})$. Then, from (10)–(11), the backstepping and adaptation laws are given by

$$\dot{\nu}_e = -\gamma_1 e_v - \alpha \nu_e$$
$$\dot{\hat{m}} = \gamma_2 e_v^T(ge_3 - \dot{V})$$

where $\gamma_1, \gamma_2 > 0$ are the control gains. With the uncertainty in m, the decoding equation (13) of the backstepping law can also be written as

$$\bar{\nu} = -\hat{m}\left(\frac{d}{dt}\left[\frac{\partial V}{\partial x}\right]\dot{x} + \frac{\partial V}{\partial x}\hat{\ddot{x}}\right) - b\left(\hat{\ddot{x}} - \dot{V}\right) - \dot{\hat{m}}(ge_3 - \dot{V})$$
$$- \alpha\left[\hat{m}\dot{V} - b(\dot{x} - V) - \hat{m}ge_3\right] + \gamma_1 e_v$$

where $\hat{\ddot{x}}$ is the acceleration estimate as obtained in (15).

This completes the design example of the passivity-based adaptive backstepping velocity field following control. Notice that the designed control satisfies all the structural properties required for Theorem 1 and Lemma 1; thus, the boundedness and convergence of $(\xi, \nu_e, \tilde{m})$ will be guaranteed under some suitable conditions as speculated in Theorem 1 and Lemma 1. Note also that the persistency of excitation condition in Theorem 1 will be granted if $Y_2(t) = ge_3 - \dot{V}$ (or, simply $\dot{V}$) is "rich" enough all the time (with $\Gamma = 1$). See also Section 5 for the experimental results of this adaptive backstepping control.

3.2. Example 2: trajectory tracking

Suppose that we want the Cartesian position x of the quadrotor (1)–(2) to track a timed-trajectory $x_d(t) \in \Re^3$. Here, we assume that $\dot{x}_d(t), \ddot{x}_d(t), \dddot{x}_d(t)$ be all bounded. Then, similar to (6), we implement the following trajectory tracking control action:

$$-\lambda Re_3 = \hat{m}ge_3 + \underbrace{\hat{m}\ddot{x}_d - b\dot{e} - ke}_{=:\nu(\hat{m},x,\dot{x},t)} + \nu_e \tag{18}$$

where $e(t) := x(t) - x_d(t)$ is the tracking error, $b, k > 0$ are damping/spring gains, and $\nu_e \in \Re^3$ is the control generation error due to the quadrotor's under-actuation. The control objective is then $(\dot{e}, e) \to 0$.

With the control action (18), the quadrotor's closed-loop Cartesian dynamics becomes

$$m\ddot{e} + b\dot{e} + ke = \tilde{m}(ge_3 - \ddot{x}_d) + \nu_e$$

where $\tilde{m} = m - \hat{m}$. This closed-loop dynamics possesses the passivity property (9) as follows. First, define $\xi = [\dot{e}; e] \in \Re^6$ and $W_1 = \frac{1}{2}\xi^T P\xi$ with

$$P := \begin{bmatrix} m & \varepsilon m \\ \varepsilon m & k + \varepsilon b \end{bmatrix} \otimes I_3$$

where $\otimes$ is the Kronecker product, $I_3 \in \Re^{3\times 3}$ is the identity matrix, and $\varepsilon > 0$ is a small number to be specified shortly.

We can then show that

$$\frac{dW_1}{dt} = -\xi^T Q\xi + (\dot{e} + \varepsilon e)^T \nu_e + \tilde{m}(\dot{e} + \varepsilon e)^T (ge_3 - \ddot{x}_d)$$

where

$$Q := \begin{bmatrix} b - \varepsilon m & 0 \\ 0 & \varepsilon k \end{bmatrix} \otimes I_3.$$

Thus, if we choose $\varepsilon > 0$ small enough s.t.,

$$0 < \varepsilon < b/m$$

P, Q will both become positive-definite, thereby, the passivity relation (9) is achieved with $y_1 = \dot{e} + \varepsilon e$ and $y_2 = (\dot{e} + \varepsilon e)^T (ge_3 - \ddot{x}_d)$. Note that y_2 also satisfies the linear parameterization condition (14) with $\Gamma = [I_3; \varepsilon I_3] \in \Re^{6\times 3}$ and $Y_2(t) = ge_3 - \ddot{x}_d \in \Re^3$.

Therefore, from (10)–(11), the backstepping and adaptation laws are given by

$$\dot{\nu}_e = -\gamma_1(\dot{e} + \varepsilon e) - \alpha\nu_e$$
$$\dot{\hat{m}} = \gamma_2(\dot{e} + \varepsilon e)^T (ge_3 - \ddot{x}_d)$$

where $\gamma_1, \gamma_2 > 0$ are the control gains. The decoding equation (13) can also be written by

$$\bar{\nu} = -\hat{m}\dddot{x}_d + b(\hat{\ddot{x}} - \ddot{x}_d) + k\dot{e} + \dot{\hat{m}}(ge_3 - \ddot{x}_d) \tag{19}$$
$$\quad - \alpha\left[\hat{m}\ddot{x}_d - b\dot{e} - ke - \hat{m}ge_3\right] + \gamma_1(\dot{e} + \varepsilon e) \tag{20}$$

where $\hat{\ddot{x}}$ is the acceleration estimate as suggested in (15).

Since this adaptive backstepping trajectory tracking control satisfies all the structural properties of Theorem 1 and Lemma 1, the boundedness and/or the convergence of $(\xi, \nu_e, \tilde{m})$ can be ensured under the conditions as given in Theorem 1 and Lemma 1. Note also that the persistency of excitation of Theorem 1 will be achieved if $Y_2(t) = ge_3 - \ddot{x}_d \in \Re^3$, or, equivalently, the desired trajectory $\ddot{x}_d$ keeps exciting the adaptation dynamics of $\tilde{m}$. See Section 4, where this adaptive backstepping trajectory tracking control is utilized as a low-level control for the problem of haptic teleoperation of a quadrotor over the Internet. See also Section 5 for some of its relevant experimental results.

4. Haptic teleoperation of quadrotor over the internet

In this section, we apply our adaptive backstepping trajectory tracking control of Section 3.2 to the recently proposed semi-autonomous teleoperation framework in [2]. For this, we also introduce a certain dynamic-extension like filter to allow our adaptive backstepping tracking control to be used with discontinuous signals received from the Internet. We also present a complete stability and collision avoidance analysis with our adaptive backstepping trajectory tracking control also included.

More precisely, at the slave side, we simulate the following first-order *kinematic* Cartesian virtual point (VP):

$$\dot{p} = \eta\bar{q}(t) - \frac{\partial\varphi_o^T}{\partial p} \tag{21}$$

where $p \in \Re^3$ is the VP's Cartesian position, $\bar{q}(t) \in \Re^3$ is the output of a smoothing filter reflecting the master device's position $q(t) \in \Re^3$ received from the digital/discontinuous Internet communication (see below), $\eta > 0$ is to match the scale difference between the master position q and the VP's velocity $\dot{p}$, and $\varphi_o(\|p - p_o\|)$ is the obstacle avoidance potential, which produces a repulsive force when p approaches the obstacle located at p_o. The adaptive backstepping trajectory control is then used to drive the quadrotor's Cartesian position x to track this VP's position p as close as possible (i.e., $p = x_d$).

Although other types of filters may be used, here, for simplicity, we use the following simple second-order filter to computed the filtered master position $\bar{q}(t)$ for (21):

$$\ddot{\bar{q}}(t) + 2b'\dot{\bar{q}}(t) + k'\bar{q}(t) = k'q(k) \tag{22}$$

where $q(k) \in \Re^3$ is the (discontinuous) master device's position $q(t) \in \Re^3$ received from the Internet at the slave reception time t_k^s, and b', k' are the filter gains. Instead of directly using discontinuous $q(k)$ for (21) (as done in [2]), here, we utilize this filtered master position $\bar{q}(t)$ and enforce $x(t) \to \bar{q}(t)$. This is necessary since, as can be seen from (19), our adaptive backstepping trajectory tracking control requires not only $p, \dot{p}$ but also $\ddot{p}, \dddot{p}$, which become ill-defined with $q(k)$ switchings at the data reception time t_k^s. Requiring such high-order derivatives of the desired trajectory is in fact common for most of the quadrotor trajectory tracking control results (e.g., [8–10,13,14]).

Suppose that $q(k)$ is bounded, which will be enforced below by using the passive set-position modulation (PSPM) technique [18]. Then, $\ddot{\bar{q}}(t), \dot{\bar{q}}(t), \bar{q}(t)$ are all bounded due to (22). We can also compute $\ddot{p}$ and $\dddot{p}$ s.t., from (21),

$$\ddot{p} = \eta\dot{\bar{q}}(t) - H_{\varphi_o}(p)\dot{p} \tag{23}$$

$$\dddot{p} = \eta\ddot{\bar{q}}(t) - H_{\varphi_o}(p)\ddot{p} - \frac{dH_{\varphi_o}(p)}{dt}\dot{p} \tag{24}$$

where $H_{\varphi_o}(p) := \left[\frac{\partial^2\varphi_o}{\partial p_i \partial p_j}\right] \in \Re^{3\times 3}$ is the Hessian of φ_o. With $p, \dot{p}, \ddot{p}, \dddot{p}$ all well-defined, now, we can apply our adaptive backstepping trajectory tracking control of Section 3.2 to enforce $x(t) \to p(t)$.

Note that, through the term $\eta\bar{q}(t)$ in (21), human users can tele-control the VP's velocity $\dot{p}$ by the master device's position $q(t)$, thereby, circumvent the problem of master–slave *kinematic dissimilarity* (i.e. stationary master's workspace is bounded, yet, that of the mobile slave quadrotor is unbounded [19,20]). The kinematic VP (21) is also adopted here as done in [2] in contrast to the dynamic VPs (e.g., [3]), since it can greatly simplify the collision avoidance analysis as shown in the next Proposition 1.

To derive Proposition 1, let us denote the ultimate bound of $\|\xi\|$ in (16) of Lemma 1 by $\xi_{\max}$ s.t., $\xi_{\max} \geq \|\xi(t)\|$ for all $t \geq 0$, where $\xi = [\dot{x} - \dot{p}; x - p]$ in this case. Let us also assume that: (1) the avoidance potential φ_o is constructed s.t.: (i) there exists a large enough $\bar{M} > 0$ s.t. $\varphi_o(\|p - p_o\|) \leq \bar{M}$ implies $\|p - p_o\| > \xi_{\max}$; and (ii) if $\varphi_o(\|p - p_o\|)$ gets very large, so does $\|\partial\varphi_o/\partial p\|$; and also (2) we set the filter coefficients b', k' of (22) to be critically damped.

Proposition 1. *Suppose $q(t)$ is bounded, i.e., $\exists q_{\max} \geq 0$ s.t. $q_{\max} \geq \|q(t)\|$ $\forall t \geq 0$. Suppose further that, if $\varphi_o(\|p - p_o\|) \geq \bar{M}$,*

$$\left\|\frac{\partial\varphi_o}{\partial p}\right\| > \eta q_{\max} \tag{25}$$

where η is the scaling factor in (21). Then, $\varphi_o \leq \bar{M}$ and $\|x - p_o\| > 0$ $\forall t \geq 0$ (i.e., no collision). Suppose further that $\partial\varphi_o^2/\partial p_i\partial p_i$ and $\partial\varphi_o^3/\partial p_i\partial p_i\partial p_k$ are bounded if $\varphi_o \leq \bar{M}$. Then, $\dot{p}, \ddot{p}, \dddot{p}$ are all bounded.

Proof. Differentiating $\varphi_o(\|p - p_o\|)$, we can have

$$\dot{\varphi}_o = \frac{\partial\varphi_o}{\partial p}\left[\eta\bar{q}(t) - \frac{\partial\varphi_o^T}{\partial p}\right] = \eta q_{\max}\left\|\frac{\partial\varphi_o}{\partial p}\right\| - \left\|\frac{\partial\varphi_o}{\partial p}\right\|^2 \tag{26}$$

where we also use the fact that the l_1-norm of the impulse response $h(t)$ of the filter equation (22) with the critically-damped (b', k') is $\|h(t)\|_1 = 1$, so that $\|\bar{q}(t)\|_{\max} = q_{\max}$. Now, suppose that, at a certain instance, $\varphi_o > \bar{M}$. At that time, however, due to the assumption (25) and the quadratic structure of (26), we must have $d\varphi_o/dt < 0$. This then implies that $\varphi_o(\|p - p_o\|) \leq \bar{M}$. Thus, we have $\|p - p_o\| > \xi_{\max}$, and, consequently, $\|x - p_o\| \geq \|p - p_o\| - \|x - p\| > \xi_{\max} - \xi_{\max} = 0$, that is, no collision. Boundedness of $\dot{p}, \ddot{p}, \dddot{p}$ can also be easily seen from their expressions (21), (23), (24), with the fact that $\dot{\bar{q}}, \ddot{\bar{q}}$ are bounded with bounded $q(t)$, since the filter itself (22) is stable. ■

With $\dot{p}, \ddot{p}, \dddot{p}$ now shown to be bounded, we may then apply the adaptive backstepping trajectory tracking control of Section 3.2 to drive the quadrotor's position x to track the VP's position p. Boundedness of $q(t)$ in Proposition 1 will also be guaranteed by applying passive set-position modulation (PSPM) technique at the master site as elucidated below.

To allow the user to perceive the presence of the obstacle and also the state (i.e., velocity) of the quadrotor, we also design the haptic feedback signal $y(t) \in \Re^3$ to be sent from the slave site to the master device, s.t.

$$y(t) := \frac{1}{\eta}\left(\dot{x} + \frac{\partial\varphi_o^T}{\partial p}\right) \tag{27}$$

where the two terms, $\dot{x}/\eta$ and $(1/\eta)\partial\varphi_o^T/\partial p$, are typically complementary, i.e., during the free cruise flying with no obstacles around, $\partial\varphi_o^T/\partial p \approx 0$, whereas during the contact with an obstacle, $\dot{x} \approx 0$.

This $y(t)$ is then sent to the master site over the Internet. Let us denote by $y(k)$ its reception at the master site over the Internet at the (master) reception time t_k^m. We incorporate this $y(k)$ into the PD-type coupling τ for the master device s.t.

$$\tau(t) := -B\dot{q} - K_1 q - K(q - \bar{y}(k)) \tag{28}$$

for $t \in [t_k^m, t_{k+1}^m)$, where $B, K_1, K \succ 0$ are diagonal gain matrices, and $\bar{y}(k)$ is a certain modulation of $y(k)$ (to be defined below). Here, the spring action K_1 is included to provide haptic feedback of $y(t)$ even when K attempts $\|q(t) - \bar{y}(k)\| \to 0$. On the other hand, the damping B is included to avoid oscillatory behavior.

If we use $y(k)$ directly in (28), the PD-coupling (28) can generally become unstable. To address this problem, as proposed in [2], we adopt here passive set-position modulation (PSPM) [18], which is more flexible (e.g., passive feedback of $y(k)$) and less conservative (i.e., selective activation of passifying action only necessary) than conventional time-invariant passivity-enforcing frameworks. More precisely, at each t_k^m, $\bar{y}(k)$ in (28) is computed s.t.

$$\min_{\bar{y}(k)} \|y(k) - \bar{y}(k)\|$$

$$\text{subj. } E(k) = E(k-1) + D_{\min}(k-1) - \Delta\bar{P}(k) \geq 0$$

where $E(k) \geq 0$ is the virtual energy reservoir;

$$\Delta\bar{P}(k) := \frac{1}{2}\left(\|q(t_k^m) - \bar{y}(k)\|_K^2 - \|q(t_k^m) - \bar{y}(k-1)\|_K^2\right)$$

is the modulated spring energy jump at t_k^m with $\|x\|_A^2 := x^T A x$; and

$$D_{\min}(k) := \frac{1}{t_{k+1} - t_k}\sum_{i=1}^{3} b_i(\bar{q}_i(k) - \underline{q}_i(k))^2$$

is the reharvesting of the (otherwise waster) energy dissipation via B, with $b_i > 0$ being the ith diagonal element of B, q_i the ith element of q, and $\bar{q}_i(k)/\underline{q}_i(k)$ the max/min of $q_i(t)$ during $[t_k, t_{k+1})$, $i = 1, 2, 3$. Note that this PSPM is implemented only for the master side. Also, since the human operator usually keeps injecting energy into the master, $E(k)$ may keep increasing as well. To avoid excessive energy accumulation in $E(k)$, we ceil off $E(k)$, by discarding any energy over a certain threshold $\bar{E}$. See [18] for more details on PSPM. The following Theorem 2 can be shown similar to [18,2]; thus, its proof is omitted here.

Theorem 2. (1) *The master device with PSPM-modulated control (28) is closed-loop passive, that is, $\exists c_1 \in \Re$ s.t., $\int_0^T f^T\dot{q}dt \geq -c_1^2$, $\forall T \geq 0$, where $f, \dot{q} \in \Re^3$ are the human force and velocity. Moreover, if the human user is passive (i.e. $\exists c_2 \in \Re$ s.t., $\int_0^T f^T \dot{q}dt \leq c_2^2$, $\forall T \geq 0$), the closed-loop VP's teleoperation system is stable, with $\dot{q}, q, q - \bar{y}(k)$, and $\dot{p}$ all bounded.*

(2) *Suppose further that $\ddot{q}, \dot{q} \to 0$, $E(k) > 0$ $\forall k \geq 0$, and $(x, \dot{x}) = (p, \dot{p})$. Then,* (a) *if $\partial\varphi_o/\partial p = 0$ (e.g. no obstacles), $f(t) \to \frac{K_1}{\eta}\dot{x}_i$ (i.e. UAV velocity perception); or* (b) *if $\dot{x} = 0$ (e.g. stopped by obstacles), $f(t) \to \frac{K_1}{\eta}\partial\varphi_o/\partial p$ (i.e. collective obstacle perception).*

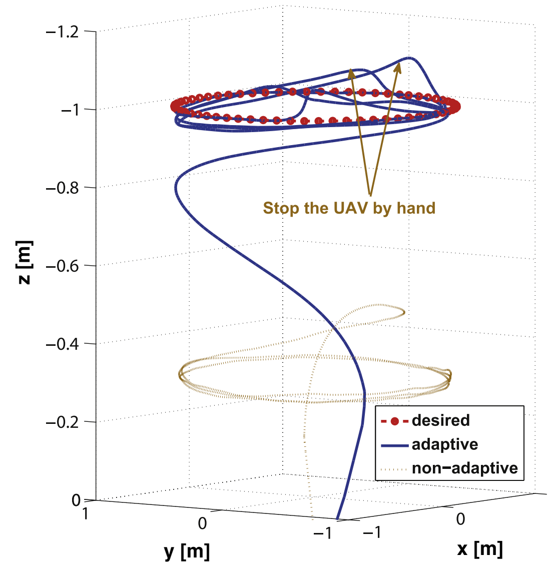

Fig. 3. Adaptive backstepping velocity field following: 3D trajectory.

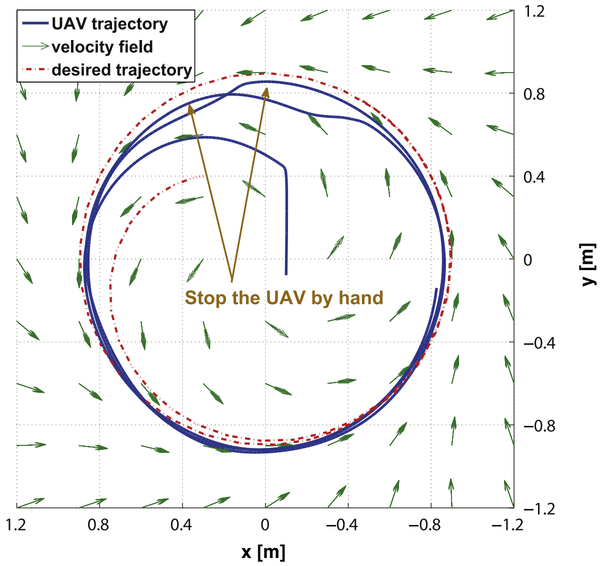

Fig. 4. Adaptive backstepping velocity field following: 2-D view of velocity field and trajectory.

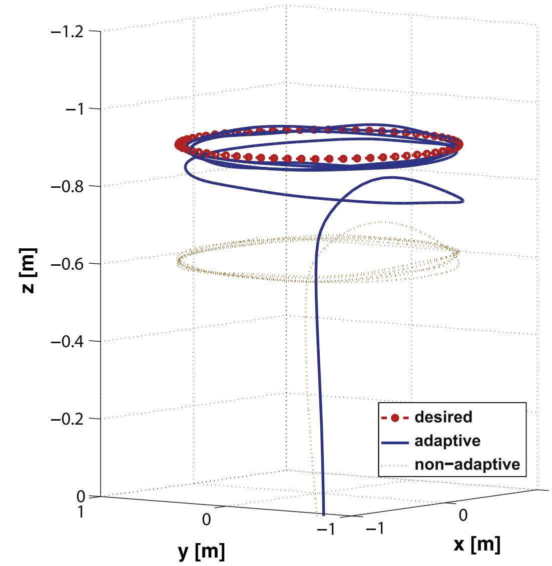

Fig. 7. Adaptive backstepping trajectory tracking: 3D trajectory.

Notice the flexibility in designing/using the haptic feedback $y(t)$ (27) provided by PSPM. Other forms of $y(t)$ can also be possible without jeopardizing passivity. How to choose this haptic feedback form $y(t)$ to maximize human perception is an interesting research topic and we spare it as a future research topic. The item (1) of Theorem 2 and Proposition 1 essentially establishes master-passivity/slave-stability of the closed-loop teleoperation system, which, we believe, would likely provide a sharper performance than (more conservative) master-passivity/slave-passivity, and also more adequate and also sufficient here, as the quadrotor interacts only with the virtual obstacle avoidance force, which is precisely known. Experimental results of this haptic teleoperation scheme are presented in Section 5.

5. Experiments

In this section we report the results of three experiments to validate the proposed adaptive backstepping control laws: ve-

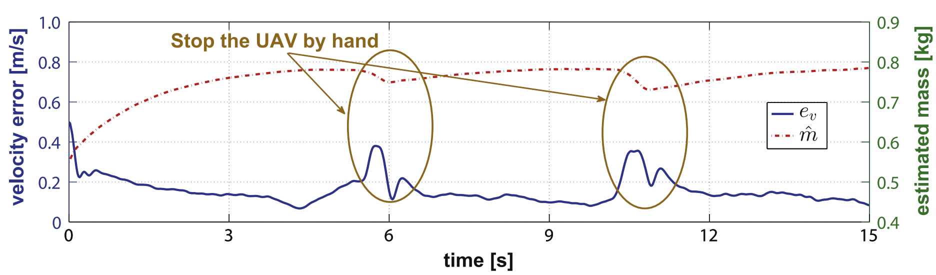

Fig. 5. Adaptive backstepping velocity field following: velocity following error and estimated mass $\hat{m}$.

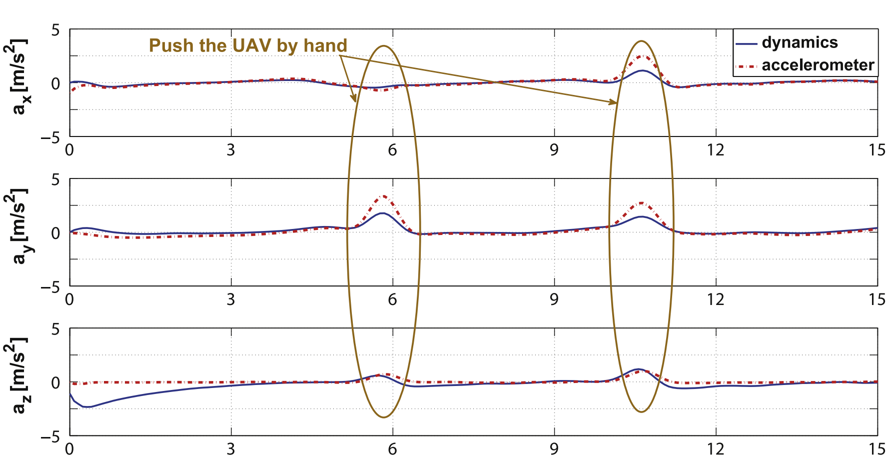

Fig. 6. Adaptive backstepping velocity field following: acceleration via dynamics equation (15) and from on-board accelerometer (low-pass-filtered).

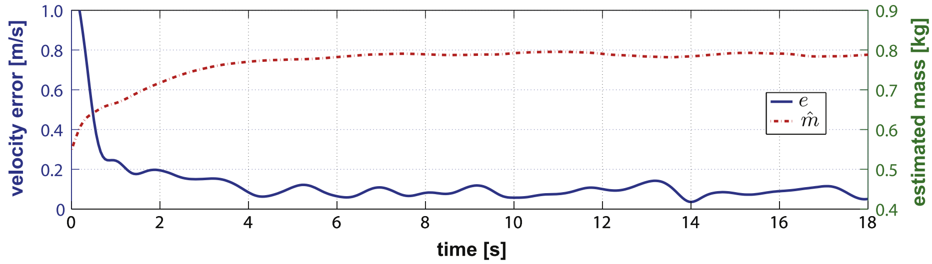

Fig. 8. Adaptive backstepping trajectory tracking: tracking error and estimated mass $\hat{m}$.

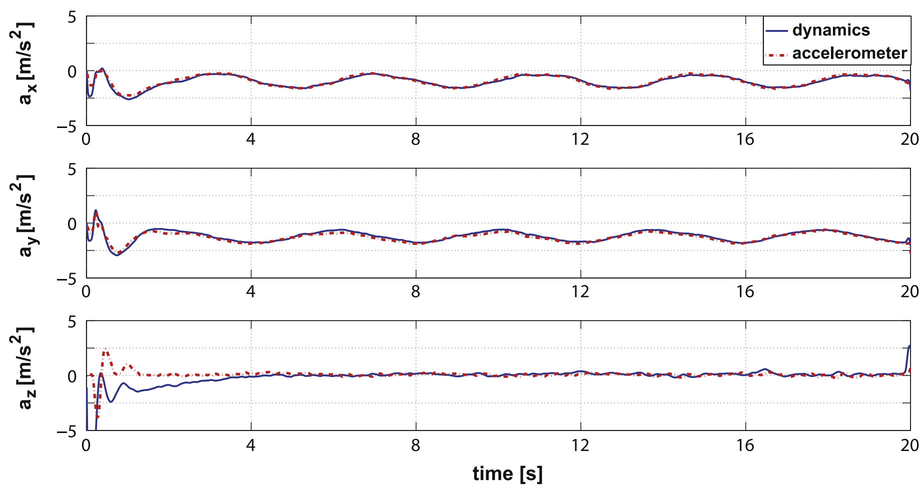

Fig. 9. Adaptive backstepping trajectory tracking: acceleration via dynamics equation (15) and from on-board accelerometer (low-pass-filtered).

locity field following, timed trajectory tracking, and its application to haptic teleoperation over the Internet. We use Ascending Technologies® Pelican as our quadrotor. Xbee, a radio module, is used to communicate with a control PC so that a human user can receive sensor information from the UAV and send control command for the thrust force and angular velocity. The quadrotor is powered by the LiPo 6000 mAh battery and its maximum velocity is 50 km/h and maximum payload is 650 g. It also has 4 brush-less motors, Atom processor board, IMU, and GPS. The real mass of the UAV is about 800 g, and we found $\hat{m}$ converges to a value similar to that. For the experiment, we use Vicon® with 8 Bonita cameras with 100 Hz to measure rotation and translation information of the quadrotor. For the teleoperation, we also used a haptic device, Force Dimension®, Omega 3, whose maximum force is 12 N, linear resolution is 0.01 mm, and rate is up to 8 kHz. In our experiment, the haptic signal is updated with 2 kHz.

5.1. Adaptive backstepping velocity field following

We define 3D velocity field that has 0.9 m radius limit cycle at the 1 m height so that the desired path make a circular trajectory at 1 m. To verify the effectiveness of adaptive control, experiment with an underestimated mass of the UAV is performed. Fig. 3 shows that the z-directional motion cannot converge to the desired height even though 2-Dimensional motion follows the desired velocity field well (Fig. 4). This shows that the adaptation is necessary to maintain the desired height. The blue solid line in Fig. 3 represents the real trajectory with adaptive control. Even if the initial mass is set to be 0.55 g, the UAV can fly at the desired height.

We also stop the UAV during the flight by hand around 5 and 11 s. One can then see from Figs. 3 and 5 that, when we push the UAV, the velocity error increases. However, after the pushing ends, the quadrotor resumes to follow the velocity field and velocity error decreases again. Fig. 6 shows the estimated acceleration using the dynamics equation (15) and that measured (and low-pass-filtered) from the on-board accelerometer. From there, we can see that the estimated acceleration matches well with the measured acceleration most of the time, except: in the beginning, where the error in the estimated mass $\hat{m}$ is significant, and at times of the human-pushing with δ in (1) not negligible anymore.

5.2. Adaptive backstepping trajectory tracking

Similarly to the previous experiment, we set the desired timed trajectory that makes a circle at a certain height. First, we set the mass as 0.55 g without adaptive control and Fig. 7 shows the result (yellow dotted line). From there, it is clear that, with no adaptation, the quadrotor cannot attain the desired height. However, with adaptive control, even though the initial mass is set to be 0.55 g, the UAV can fly along the desired trajectory at the desired height (blue solid line).

The position error $e := x - x_d$ converges to less than 0.1 m with the proposed adaptive backstepping control and the estimated mass $\hat{m}$ also converges to a stationary value (Fig. 8). This trajectory tracking motion is more aggressive than that of the above velocity field following as shown in Fig. 9, from which we can also see that our estimated acceleration obtained using dynamics equation (15) is adequate even for this fast motion.

5.3. Haptic teleoperation over the internet

In this experiment, we teleoperated the UAV over the imperfect Internet communication with time varying delay and packet loss.

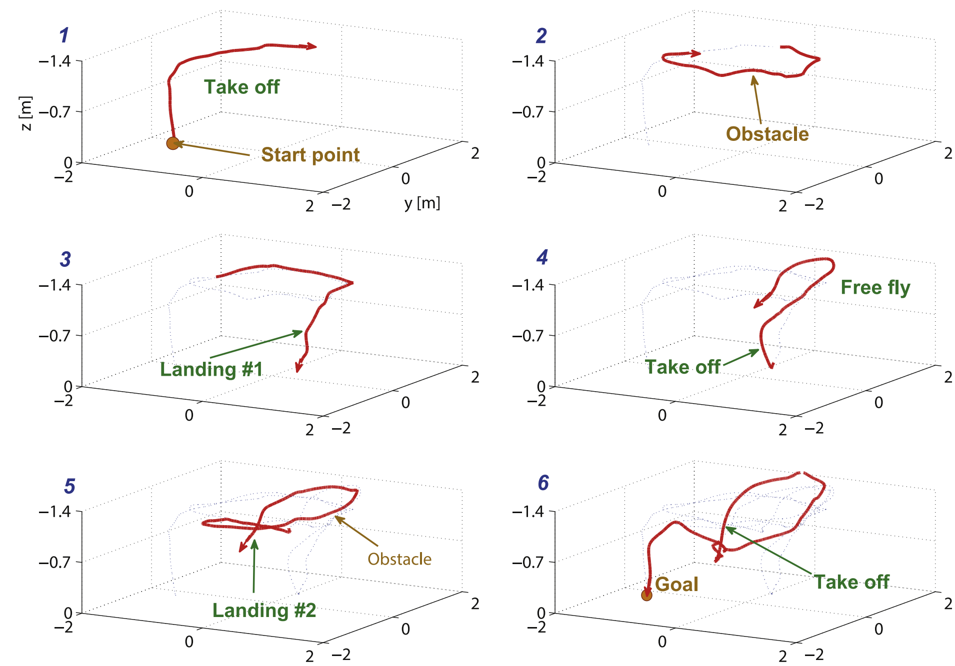

Fig. 10. UAV trajectory using the haptic teleoperation with imperfect communication.

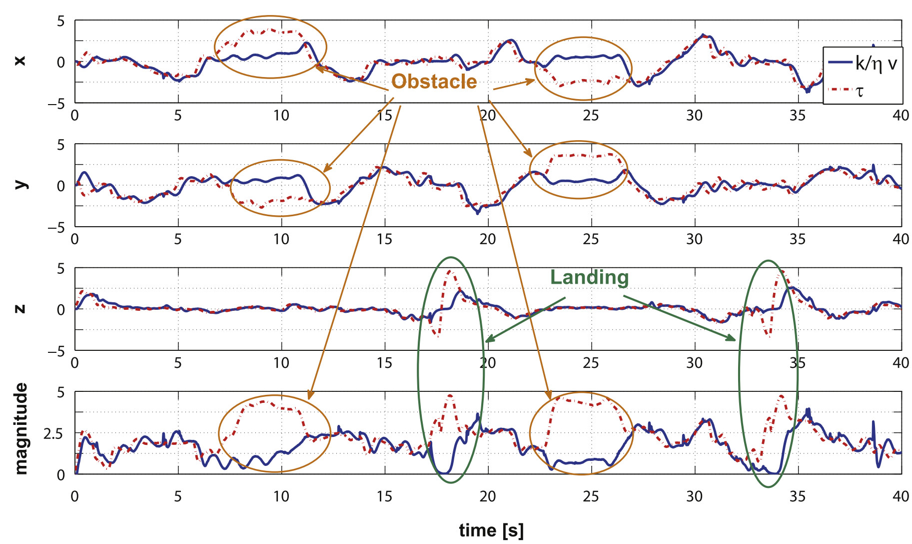

Fig. 11. Haptic teleoperation of UAV with delay varying from 20 to 60 ms.

The task goes as shown in Fig. 10: (1) at the beginning, the human user starts at a certain position; (2) during the flight, user should touch and feel an obstacle, which is located at the center of the workspace; (3) the user then lands the quadrotor on the specifically determined location #1; (4) if the user succeeds the first landing, he starts to go to the next landing site #2; (5) during this flight, the user again should touch and feel the obstacle before the next landing; (6) after finishing all tasks including the second landing to the site #2, the user operates the quadrotor to return to the start point.

For this task scenario, we set the communication characteristics as follows. For the first experiment, delay varies between 20 and 50 ms with the mean 35 ms, standard deviation 6.1 ms, and the data loss rate 59.62%. Fig. 11 shows the result of the first experiment. The haptic force feedback converges to the scaled velocity $(K_1/\eta\dot{x})$ at the steady-state as speculated in Theorem 2. When the UAV approaches the obstacle, the user can feel the repulsive force from the obstacle. At 10 and 25 s, the quadrotor touches the obstacle and there appears force feedback peaks showing that the user can feel the obstacle. During two landing tasks, the force peak is because the user should push down the haptic device to land the quadrotor.

In the second experiment, the delay varies between 400 and 600 ms, with the mean 500.1 ms, standard deviation 40.8 ms, and loss rate is 81.24%. Even though the user performed the same task, it takes 15 s more than the previous experiment because of the longer delay and higher loss rate. It is particularly harder for the user to precisely tele-control the quadrotor's position so that the landing tasks becomes more difficult than the first experiment. The more prominent fluctuations in Fig. 12 represent this difficulty even in steady-state.

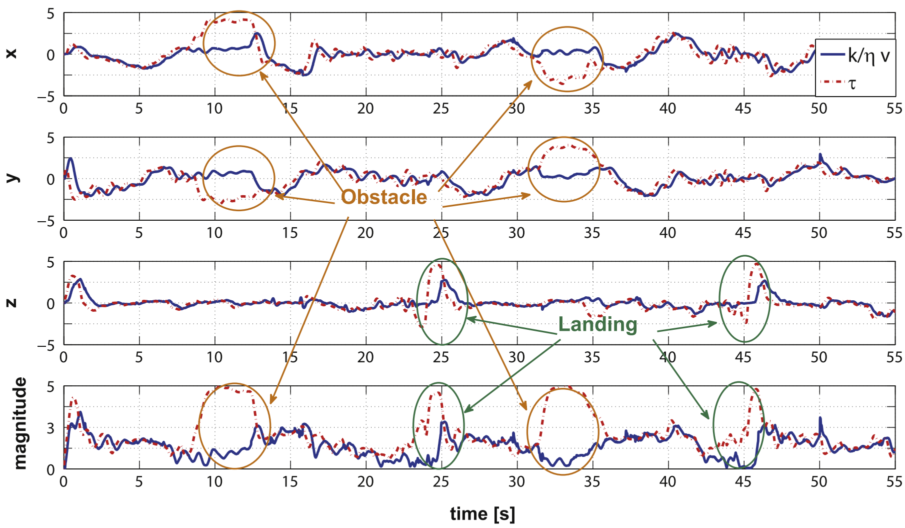

Fig. 12. Haptic teleoperation of UAV with delay varying from 400 to 600 ms.

6. Conclusions

In this paper, we propose a novel unified passivity-based adaptive backstepping control framework for under-actuated "mixed" quadrotor-type UAVs, which accepts 1-DOF thrust force input and 3-DOF angular velocity input. The backstepping technique is used to overcome the issue of the quadrotor's under-actuation, while the adaptive control approach to real-time estimate uncertain mass parameter of the quadrotor. Its two examples, velocity field following control and trajectory tracking control, are also worked out. Its application to haptic teleoperation over the Internet is also presented with dynamic-extension like filter to address discontinuous Internet communication and a complete stability/collision-avoidance analysis provided. Experiments are also performed to show the efficacy of the proposed theoretical results.

Some future research directions include: (1) elucidation of a relation between the passivity condition (9) and the differential-flatness of quadrotors [21]; (2) extension to more general classes of under-actuated systems; and (3) perceptually-optimized design of haptic signal $y(t)$ in (27) and further human-subject study for teleoperation with lossy-communication.

References

[1] V. Kumar, N. Michael, Opportunities and challenges with autonomous micro aerial vehicles, in: Proc. of Int'l Symposium on Robotics Research, 2011.
[2] D.J. Lee, A. Franchi, H.-I. Son, C. Ha, H.H. Bülthoff, P.R. Giordano, Semi-autonomous haptic teleoperation control architecture of multiple unmanned aerial vehicles, IEEE/ASME Trans. Mechatronics 18 (4) (2013) 1334–1345.
[3] S. Stramigioli, R. Mahony, P. Corke, A novel approach to haptic tele-operation of aerial robot vehicles, in: Proc. IEEE Int'l Conf. on Robotics & Automation, 2010, pp. 5302–5308.
[4] C. Ha, D.J. Lee, Vision-based teleoperation of unmanned aerial and ground vehicles, in: Proc. IEEE Int'l Conference on Robotics & Automation, 2013, pp. 1457–1462.
[5] D.J. Lee, Distributed backstepping control of multiple thrust-propelled vehicles on balanced graph, Automatica 48 (11) (2012) 2971–2977.
[6] R. Sepulchre, M. Jankovic, P. Kokotovic, Constructive Nonlinear Control, Springer-Verlag, London, 1997.
[7] J.J.E. Slotine, W.P. Li, Applied Nonlinear Control, Prentice Hall, Englewood Cliffs, NJ, 1991.
[8] E. Frazzoli, M.A. Dahleh, E. Feron, Trajectory tracking control design for autonomous helicopters using a backstepping algorithm, in: Proc. American Control Conference, 2000, pp. 4102–4107.
[9] R. Mahony, T. Hamel, Robust trajectory tracking for a scale model autonomous helicopter, Internat. J. Robust Nonlinear Control 14 (2004) 1035–1059.
[10] A.P. Aguiar, J.P. Hespanha, Trajectory-tracking and path-following of under-actuated autonomous vehicles with parametric modeling uncertainty, IEEE Trans. Automat. Control 52 (8) (2007) 1362–1379.
[11] P. Castillo, A. Dzul, R. Lozano, Real-time stabilization and tracking of a four-rotor mini rotocraft, IEEE Trans. Control Syst. Technol. 12 (4) (2004) 510–516.
[12] S. Bouabdallah, R. Siegwart, Backstepping and sliding-mode techniques applied to an indoor micro quadrotor, in: Proc. IEEE Int'l Conf. on Robotics & Automation, 2005, pp. 2259–2264.
[13] M.-D. Hua, T. Hamel, P. Morin, C. Samson, A control approach for thrust-propelled underactuated vehicles and its application to VTOL drones, IEEE Trans. Automat. Control 54 (8) (2009) 1837–1853.
[14] A. Roberts, A. Tayebi, Adaptive position tracking of VTOL UAVs, IEEE Trans. Robot. 27 (1) (2011) 129–142.
[15] D.J. Lee, C. Ha, Z. Zuo, Backstepping control of quadrotor-type UAVs and its application to teleoperation over the Internet, in: S. Lee, H. Cho, K.-J. Yoon, J. Lee (Eds.), Intelligent Autonomous Systems 12, in: Advances in Intelligent Systems & Computing, vol. 194, Springer, Berlin, Heidelberg, 2013, pp. 217–225.
[16] M.W. Spong, S. Hutchinson, M. Vidyasaga, Robot Modeling and Control, John Wiley & Sons, Hoboken, NJ, 2006.
[17] H.K. Khalil, Nonlinear Systems, second ed., Prentice-Hall, Upper Saddle River, NJ, 1995.
[18] D.J. Lee, K. Huang, Passive-set-position-modulation framework for interactive robotic systems, IEEE Trans. Robot. 26 (2) (2010) 354–369.
[19] D.J. Lee, O. Martinez-Palafox, M.W. Spong, Bilateral teleoperation of a wheeled mobile robot over delayed communication networks, in: Proc. IEEE Int'l Conf. on Robotics & Automation, 2006, pp. 3298–3303.
[20] Z. Zuo, D.J. Lee, Haptic tele-driving of a wheeled mobile robot over the Internet: a PSPM approach, in: Proc. IEEE Conference on Decision & Control, 2010, pp. 3614–3619.
[21] D. Mellinger, N. Michael, V. Kumar, Trajectory generation and control for precise aggressive maneuvers with quadrotors, in: Proc. of Int'l Symposium on Experimental Robotics, 2010.

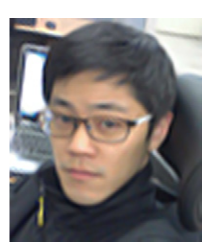

ChangSu Ha received the B.S. degree from the Sungkyunkwan University, Suwon, Korea, 2002, and the M.S. degree from the Seoul National University, Seoul, Korea, 2013, both in mechanical engineering. He is currently working toward his Ph.D. degree in mechanical engineering at the Seoul National University. His research interests include Internet teleoperation and control of flying robots.

Zhiyuan Zuo received the B.E. degree in automotive engineering from the Harbin Institute of Technology, China, 2009, and the M.S. degree in mechanical engineering from the University of Tennessee–Knoxville, 2011. He is currently a Hardware Engineer with Schneider Electric, China. He research interests include human–robot interaction, mobile robots, teleoperation and mechatronics.

Francis B. Choi received the B.S. degree in mechanical engineering from the Seoul National University, 2013, and currently working toward his M.S.-Ph.D. degree at the same university. His research interests include the design, control, and teleoperation of aerial robots, and multi-robot system control.

Dongjun Lee is an Associate Professor with the Department of Mechanical and Aerospace Engineering at the Seoul National University. He received the B.S. and M.S. degrees from KAIST, Korea, and the Ph.D. degree in mechanical engineering from the University of Minnesota, respectively in 1995, 1997 and 2004. He was an Assistant Professor with the Department of Mechanical, Aerospace and Biomedical Engineering at the University of Tennessee, 2006–2011, and a Postdoctoral Researcher with the Coordinated Science Laboratory at the University of Illinois at Urbana-Champaign, 2004–2006. His main research interests are dynamics and control of robotic and mechatronic systems with emphasis on teleoperation/haptics, multirobot systems, aerial robots, and geometric mechanics control theory. Dr. Lee received the US NSF CAREER Award in 2009, the Best Paper Award from the IAS-2012, and the 2002–2003 Doctoral Dissertation Fellowship of the University of Minnesota. He is an Associate Editor of the IEEE Transactions on Robotics.